

Optical Properties of $\text{Si}_{1-x}\text{Ge}_x$ Quantum Wells and Superlattices Grown by Rapid Thermal Chemical Vapor Deposition

J.C. Sturm, X. Xiao, H. Manoharan and P.V. Schwartz

Department of Electrical Engineering
Princeton University
Princeton, NJ 08544

Abstract

Through proper reactor design and accurate temperature measurement, high quality silicon/silicon-germanium alloy ($\text{Si}_{1-x}\text{Ge}_x$) strained layer structures can be grown by Rapid Thermal Chemical Vapor Deposition with growth temperatures in the 600-700 °C range. Photoluminescence measurements show well resolved band-edge features, indicating that the films are of very high quality. Quantum confinement effects have also been observed in quantum wells with widths down to 3 nm.

Introduction

The silicon/silicon-germanium alloy ($\text{Si}/\text{Si}_{1-x}\text{Ge}_x$) material system is of great technological interest since it offers the possibility of "band gap engineering" in silicon-based semiconductor devices. This paper discusses the growth of such structures by the Rapid Thermal Chemical Vapor Deposition (RTCVD) growth technique, and then describes the photoluminescence properties of Si/SiGe quantum wells and superlattices grown by RTCVD.

The growth of high quality heterostructures in the Si/Ge material system is inherently difficult because of the 4% lattice mismatch between Si and Ge . This mismatch is almost linearly reduced as the composition of a random alloy of $\text{Si}_{1-x}\text{Ge}_x$ is changed from $x = 1.0$ (Ge) to 0 (Si). For layers which are sufficiently thin or contain low amounts of Ge , the lattice mismatch can be accommodated by growing a strained $\text{Si}_{1-x}\text{Ge}_x$ film which is under 2-D compression [1]. In this state, the lattice constant perpendicular to the growth direction is the same in the $\text{Si}_{1-x}\text{Ge}_x$ film and the silicon substrate. In this way, misfit dislocations, which are potentially harmful to devices through their scattering or trapping properties, can be avoided. Subsequent Si layers grown on top of the strained $\text{Si}_{1-x}\text{Ge}_x$ layers will have a lattice constant matching that of the original substrate, and hence will not be strained. These $\text{Si}/\text{strained Si}_{1-x}\text{Ge}_x$ structures are the focus of this paper.

Growth

For the high quality growth of $\text{Si}_{1-x}\text{Ge}_x$ strained layers by chemical vapor-deposition, several factors must be considered. First to enable the growth of metastable strained films above the equilibrium critical thickness for misfit dislocation formation, low growth temperature are required [1,2]. Second, low temperatures are also required to suppress 3-D growth tendencies to yield layers with a flat (2-D) surface [1]. For layers with $\sim 20\%$ Ge, this requires a growth temperature of less than $\sim 650^\circ\text{C}$. At such low growth temperatures, the increased stability of oxygen and water vapor on silicon surfaces [3] means that very careful reactor design and high purity techniques are required to avoid high oxygen levels in the grown films. Finally, at low temperatures, CVD growth rates are governed by the surface reactions, which are extremely temperature sensitive. For example, near 700°C , a temperature change of $\sim 30^\circ\text{C}$ can lead to a factor of 2 change in growth rate. Therefore, very accurate control of the wafer temperature is required.

These concerns have been addressed through the construction of a special RTCVD reactor for Si/Si-Ge growth [4]. The reactor basically consists of a 175mm-diameter quartz tube, in which a 100 mm Si wafer is mounted on quartz pins. The wafer is heated by a 70 kW bank of tungsten-halogen lamps located outside the reaction chamber. The vacuum system consists of a mechanical rotary vane pump. Viton O-ring seals are used, although double seals are used where feasible. Wafers are loaded into the reactor through a load-lock chamber, so that the reactor chamber is not exposed to atmospheric pressure. With this system, low oxygen levels ($< 10^{18}\text{ cm}^{-3}$) have been routinely achieved without UHV techniques.

Typical source gases are dichlorosilane and germane, and a hydrogen carrier gas is used. A high purity hydrogen source was also found to be essential for obtaining low oxygen levels. Typical growth temperatures for the $\text{Si}_{1-x}\text{Ge}_x$ layers were in the $600 - 625^\circ\text{C}$ range, and a relatively high growth of 10's of nm/min was possible because of a fortuitous catalytic reaction [5,6]. To achieve a reasonable silicon growth rate ($\sim 3\text{ nm/min}$), 700°C was used for Si growth. Therefore when switching from Si to SiGe growth (or vice versa), the silicon wafer temperature was changed from 700 to 625°C (or vice versa). The growth of individual layers was started and stopped by switching the gas flows as in conventional CVD, not the wafer temperature as in Limited Reaction Processing [7].

To accurately measure the wafer temperature, the infrared transmission technique [8,9] as shown in Fig. 1 was used. In brief, the infrared absorption of the silicon substrate is monitored in-situ to obtain the wafer temperature. Fig. 2 shows the strong dependence of this transmitted signal vs. temperature for a bare $450\ \mu\text{m}$ substrate and for a substrate on which $\sim 54\text{ nm}$ of $\text{Si}_{0.7}\text{Ge}_{0.3}$ has been grown. To measure a temperature to $\sim 1^\circ\text{C}$, a relative accuracy of a few percent in absolute transmission is required. Also, as seen in Fig. 2, the growth of thin $\text{Si}_{1-x}\text{Ge}_x$ layers has no significant effect on the technique. Note that no uncertain parameters such as emissivity are required to obtain the temperature. Using this method of temperature measurement, Fig. 3 shows the temperature vs. time characteristics that can be achieved. For the growth of a Si/ $\text{Si}_{1-x}\text{Ge}_x$ superlattice, the Si layers would be grown at the 700°C portion of the temperature profile, and the $\text{Si}_{1-x}\text{Ge}_x$ layers at the 625°C portion. The cross section TEM of such a superlattice (50 periods, $22\text{A} - \text{Si}/23\text{A} - \text{Si}_{0.8}\text{Ge}_{0.2}$) is shown

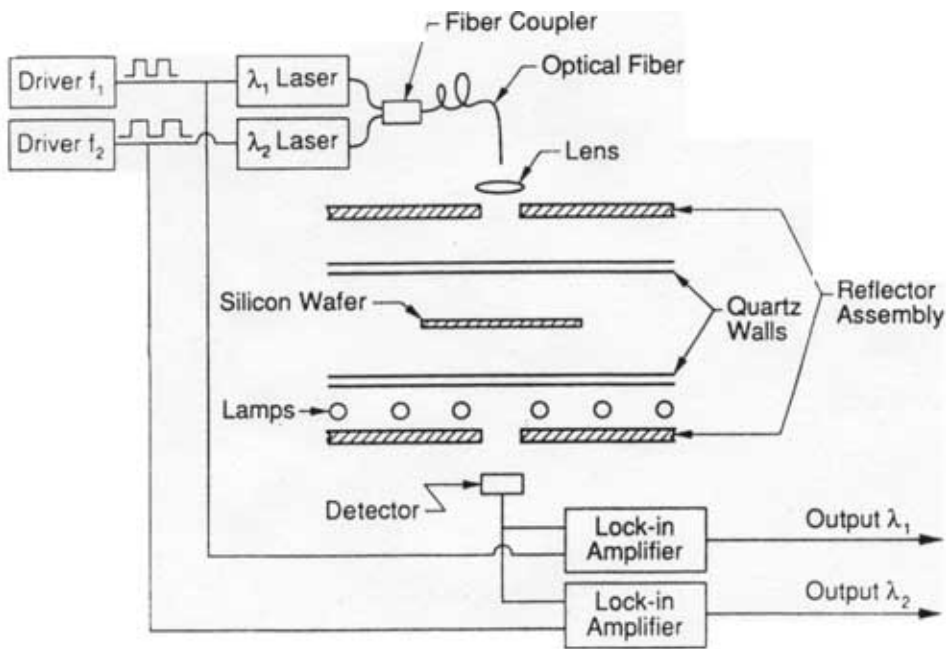


Fig. 1. Schematic cross section of RTCVD reactor with temperature control by infrared transmission.

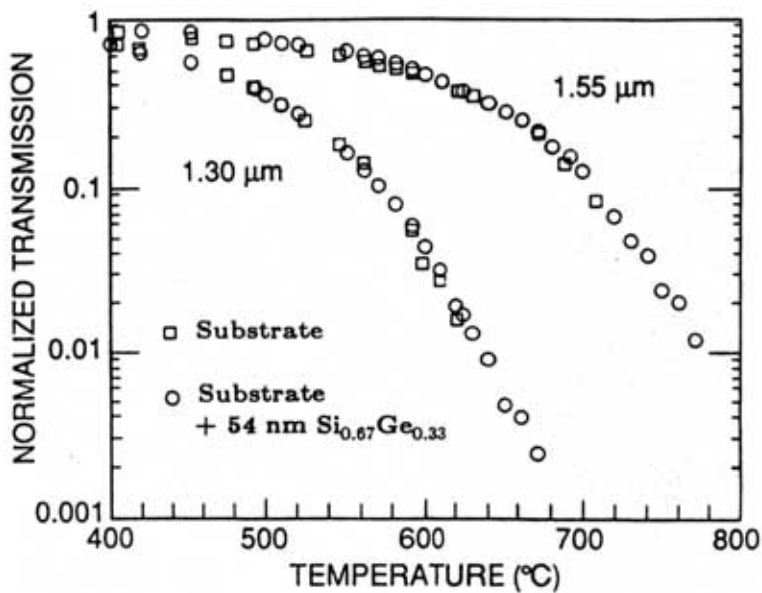


Fig. 2. High temperature infrared transmission (normalized by room temperature transmission) at 1.3 and 1.55 μm for a silicon substrate (450 μm) and the substrate with 54 nm of strained $\text{Si}_{0.67}\text{Ge}_{0.33}$.

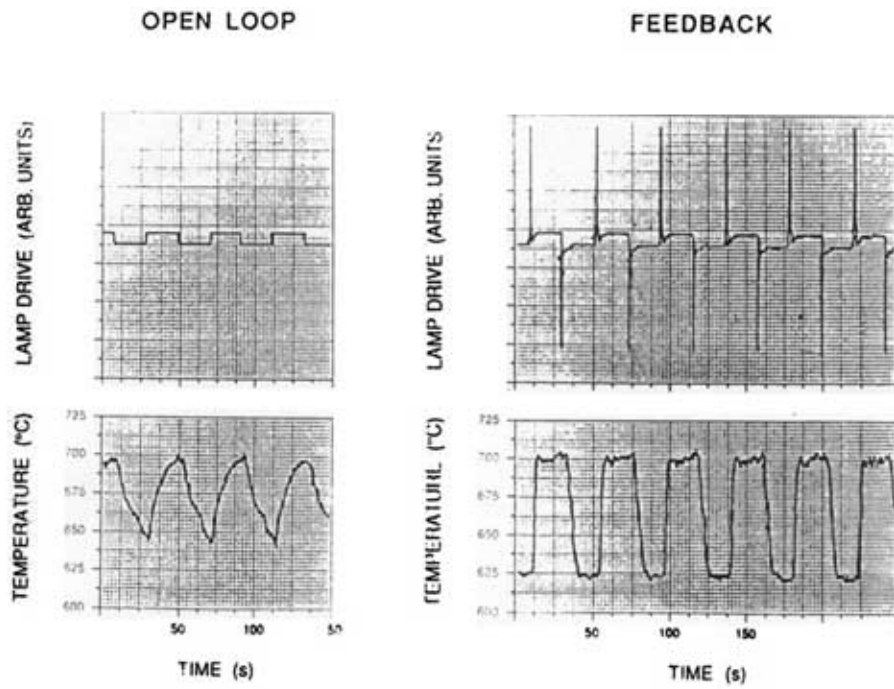


Fig. 3. Temperature vs. time profiles obtained in a) open loop control (changing lamp drive signal) and b) closed loop using I-R transmission (changing set point).

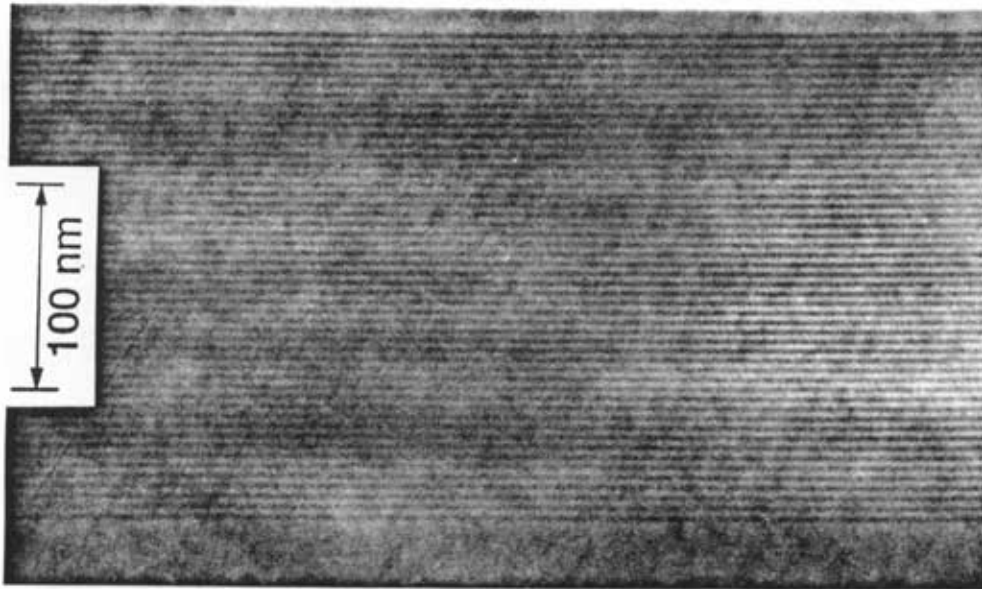


Fig. 4. Cross section TEM of a 50 period Si/Si_{0.8}Ge_{0.2} superlattice.

in Fig. 4. The individual layers are clearly resolvable, putting an upper limit on the interface abruptness of ~ 1 nm. Furthermore, the period varies by less than 5% from bottom to top, implying that the growth temperatures were maintained with an accuracy of $\leq 2^\circ\text{C}$ over 100 temperature switches.

Photoluminescence Properties

Photoluminescence (PL) is a basic technique for characterizing semiconductor films. It is especially relevant for $\text{Si}_{1-x}\text{Ge}_x$ since there is great interest in the development of $\text{Si}_{1-x}\text{Ge}_x$ optoelectronic devices such as light emitters. The most significant previous work in the luminescence of $\text{Si}_{1-x}\text{Ge}_x$ includes that in MBE samples of Noël et al. [10], where a broad band of emission well below the bandgap (peak = $E_g - 120$ meV) with efficiency as high as 10% (compared to typical $\sim 10^{-3}$ % in silicon) was observed. The mechanism for such light emission below the bandgap is not at all known at present, however, and may be due to defects. Although $\text{Si}_{1-x}\text{Ge}_x$ is an indirect bandgap semiconductor, it has been predicted that certain short period superlattices of Si/Ge will have a direct bandgap [11], with possible experimental evidence given by Zachai et al. [12]. These samples had very high misfit dislocation densities however ($10^8 - 10^{10} \text{ cm}^{-2}$), and the observed emission may have been related to dislocations and not a true measure of zone-folding. Finally, Weber et al. have carefully studied band-edge luminescence in thick uniform unstrained $\text{Si}_{1-x}\text{Ge}_x$ layers [13], but not in strained layers or in quantum well structures. The only previous report of band-edge luminescence in strained structures has been for a Ge content of only $x = 0.04$ [14].

A typical low temperature (2K) photoluminescence spectra of a sample consisting of 10 Si/strained $\text{Si}_{0.82}\text{Ge}_{0.18}$ /Si quantum wells grown by RTCVD is shown in Fig. 5(a) [15]. The samples are fully strained and have a threading defect density of $\leq 10^3 \text{ cm}^{-2}$. Because of the narrower bandgap of the $\text{Si}_{1-x}\text{Ge}_x$ layers, generated carriers are collected mostly in the $\text{Si}_{1-x}\text{Ge}_x$ quantum layers so the luminescence signal originates from these layers. The spectra contains several features which have been identified as follows. First, the highest energy peak corresponds to a no-phonon (NP) recombination mechanism, which is allowed in the indirect material because of the alloy randomness [13,15]. Such a signal would not be observed in pure Si or Ge. Below the NP peak several phonon replicas are observed, labelled transverse acoustic (TA) and transverse optical (TO). They are separated from the NP peak by their respective phonon energies. Note that the TO signal is not a single peak as it is in silicon, but is divided into 3 peaks. This is because the TO branch of the phonon dispersion curve represents primarily nearest neighbor interactions, of which three exist in the alloy (Si-Si, Si-Ge, and Ge-Ge). Because of the different bond stiffnesses and atomic masses, different phonon energies result for the three modes.

While the signal at 2K is due to bound excitons [15], the PL at 77K is due to free excitons (Fig. 5b). The spectra are basically similar, except that because of thermal broadening only the NP peak and a single TO peak are visible. Note that because it is due to alloy effects and not to localization of the excitons, the NP peak does not disappear above 20K as the excitons become free. Fig. 6 shows the PL spectrum of a 50 period 22\AA -Si/ 23\AA - $\text{Si}_{0.8}\text{Ge}_{0.2}$ superlattice, where again the structure is fully strained without dislocations.

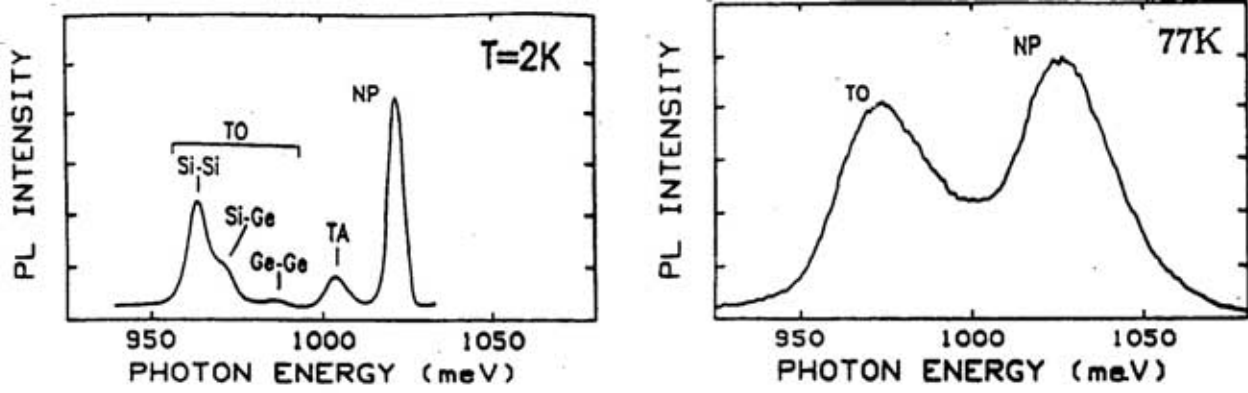


Fig. 5. Photoluminescence spectra of a 10 quantum well (30\AA of $\text{Si}_{0.82}\text{Ge}_{0.18}$) structure at a) 2K and b) 77K.

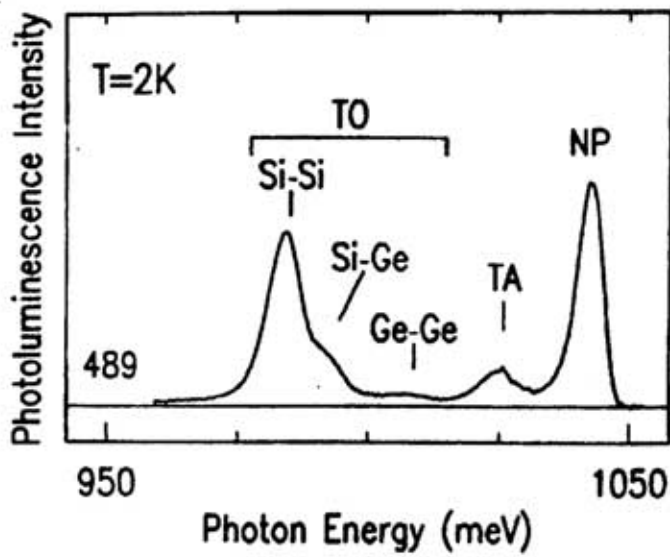


Fig. 6. PL spectrum at 2K of the 50 period superlattice of Fig. 4.

Although the spectra is shifted to higher energy because of the narrower $\text{Si}_{1-x}\text{Ge}_x$ well widths, no special features due to the superlattice are evident.

Because no corrections due to phonon energies are required, the NP PL peak provides a very sensitive probe of the bandgap, having a resolution on the order of 1 mV. This can be used to examine the quantum confinement effects which occur in a single strained $\text{Si}_{1-x}\text{Ge}_x$ quantum well. As the well width is decreased, the energy of the ground state will be increased by quantum confinement effects. Because the bandgap offset in the Si/strained $\text{Si}_{1-x}\text{Ge}_x$ system is mostly in the valence band [16], the quantum effects occur mostly on the hole energy. In Fig. 7, the effect of the width of a single strained $\text{Si}_{0.8}\text{Ge}_{0.2}$ well on the PL spectra is shown. As the well width is narrowed from 50 to 3 nm, a 45 meV shift in the spectra to higher energies is observed. Fig. 8 shows the shift in the bandgap (as measured by the NP PL signal) as a function of the well width. The results are in good agreement with the theoretical shifts predicted by band structure calculations, also shown in the figure. Although the valence band structure in strained $\text{Si}_{1-x}\text{Ge}_x$ layers is far from simple, to first order these results may also be modelled by a simple parabolic band in the $\text{Si}_{0.8}\text{Ge}_{0.2}$ with an effective mass in the growth direction of 0.3 m_0 .

Compared to samples grown by MBE, the PL results shown here indicate the superior quality of the RTCVD layers. The well-resolved band-edge PL features described above were not previously observed in strained $\text{Si}_{1-x}\text{Ge}_x$ layers grown by any other technique for more than 4% Ge. The low-temperature NP linewidth of 4 meV is near the narrowest linewidth reported for thick unstrained films [13], indicating the uniformity of the layers. MBE grown samples either exhibit no luminescence at all, or a deep signal well below the bandgap. These MBE results suggest a high concentration of deep levels that are non-radiative lifetime killers or some radiative deep level structure, respectively. In either case, these deep levels pull carriers out of the valence or conduction band, leaving few carriers to give rise to band-edge luminescence. The fundamental reason for the superior quality of the RTCVD layers over the MBE films is not known. The absence in RTCVD of a substrate heater assembly, which could cause metallic contamination problems, may be one significant advantage. The superior quality of CVD techniques in general (RTCVD or UHVCVD) for device applications has already been demonstrated [17,18] and lifetimes in the μs range have been measured in RTCVD films with low oxygen concentrations [19]. It should also be noted, however, that RTCVD $\text{Si}_{1-x}\text{Ge}_x$ films with intentionally-introduced high oxygen concentrations ($10^{19} - 10^{20} \text{ cm}^{-3}$) exhibited no luminescence, indicating that high oxygen levels lead to a reduced lifetime.

Conclusion

High quality strained $\text{Si}_{1-x}\text{Ge}_x$ layers can be grown on silicon substrates by RTCVD with an interface abruptness of < 1 nm. Key growth issues are a high purity system, a low growth temperature, and accurate temperature control. RTCVD allows one to optimize the growth temperature of each layer in a multilayer structure. The well-resolved band-edge photoluminescence observed in quantum wells and superlattices grown by RTCVD has not been observed in films grown by other techniques, and indicates the high quality of the

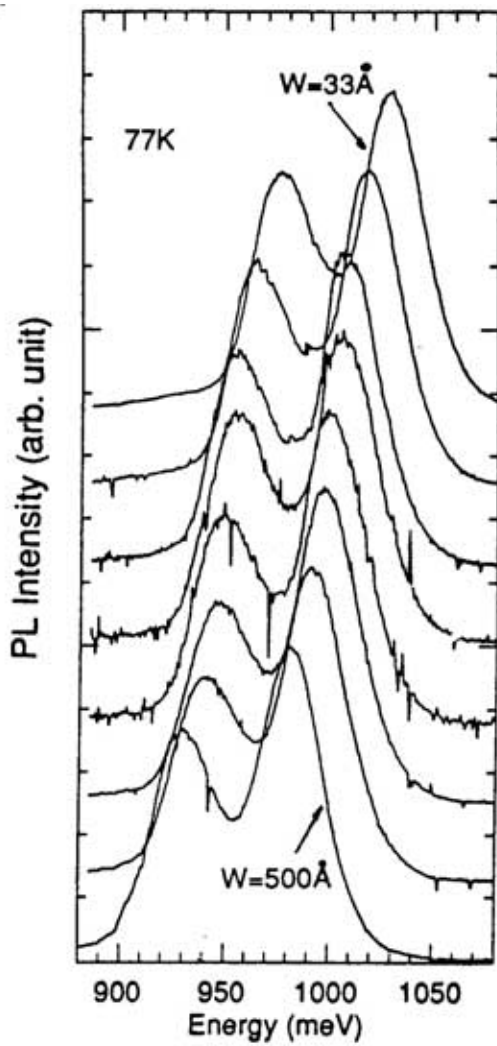


Fig. 7. 77K PL spectra of single strained $\text{Si}_{0.8}\text{Ge}_{0.2}$ quantum wells, with well widths ranging from 3.3 to 50 nm.

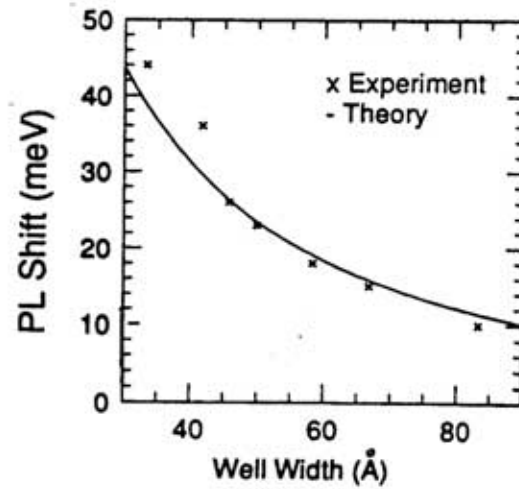


Fig. 8. Quantum confinement shift of the bandgap as a function of well width for the samples of Fig. 7, measured as a shift in the NP PL energy.

RTCVD films. Characteristic features of the band-edge luminescence are a no-phonon peak and a three-fold splitting of the transverse optical phonon replica.

Acknowledgements

Various parts of this work were done in collaboration with L. Lenchyshyn and M.L.W. Thewalt of Simon Fraser University, D.C. Houghton, N. Rowell, J.P. Noël, and J. McCaffrey of NRC, Canada, and R. Gregory and P. Fejes of Motorola. The support of NSF, ONR and the N.J. Commission on Science and Technology is gratefully acknowledged.

References

1. J.C. Bean, L.C. Feldman, A.T. Firoy, S. Nakahara and I.K. Robinson, *J. Vac. Sci. Tech.* **A2**, 436 (1984).
2. E. Kasper, H.J. Herzog, H. Jorke, and G. Abstreiter, *Proc. Symp. Mat. Res. Symp.* **102**, 393 (1988).
3. G. Ghidini and F.W. Smith, *J. Electrochem. Soc.* **131**, 2924 (1984).
4. J.C. Sturm, P.V. Schwartz and E.J. Prinz, *J. Vac. Sci. Tech.* **B9**, 2011 (1991).
5. B.S. Meyerson, K.J. Uram and F.K. Legoues, *Appl. Phys. Lett.* **53**, 2555 (1988).
6. P.M. Garone, J.C. Sturm, P.V. Schwartz, S.A. Schwartz and B. Wilkens, *Appl. Phys. Lett.* **56**, 1275 (1990).
7. J.F. Gibbons, C.M. Gronet and K.E. Williams, *Appl. Phys. Lett.* **47**, 721 (1985).
8. J.C. Sturm, P.M. Garone and P.V. Schwartz, *J. Appl. Phys.* **69**, 542 (1991).
9. J.C. Sturm, P.V. Schwartz and P.M. Garone, *Appl. Phys. Lett.* **56**, 961 (1990).
10. J.P. Noël, N.L. Rowell, D.C. Houghton and D.D. Perovic, *Appl. Phys. Lett.* **57**, 1037 (1990).
11. U. Gnutzmann and K. Clausecker, *Appl. Phys.* **3**, 9 (1974).
12. R. Zachai, K. Eberl, G. Abstreiter, E. Kasper and H. Kibbel, *Phys. Rev. Lett.* **64**, 1055 (1990).
13. J. Weber and M.I. Alonso, *Phys. Rev.* **B40**, 5683 (1989).
14. K. Terashima, M. Tajima and T. Tatsumi, *Appl. Phys. Lett.* **57**, 1925 (1990).
15. J.C. Sturm, H. Manoharan, L.C. Lenchyshyn, M.L.W. Thewalt, N.L. Rowell, J.P. Noël and D.C. Houghton, *Phys. Rev. Lett.* **66**, 1362 (1991).
16. R. People, *Phys. Rev.* **B32**, 1405 (1985).
17. G.L. Patton, D.L. Harame, J.M.C. Stork, B.S. Meyerson, G.J. Scilla and E. Ganin, *IEEE Elec. Dev. Lett.* **EDL-10**, 534 (1989).
18. J.C. Sturm and E.J. Prinz, *IEEE Elec. Dev. Lett.* **EDL-12**, 303 (1991).
19. P.V. Schwartz and J.C. Sturm, *Appl. Phys. Lett.* **57**, 2004 (1990).